Study on the mechanisms underlying the biological effects of extremely low frequency electromagnetic fields (ELF EMFS) on a fibroblast model.

E. Sereni[1], P. Faraoni[2], A. Gnerucci[2], F. Cialdai[1], M. Monici[1], F. Ranaldi[2]

[1] ASAcampus Joint Laboratory, ASA Res. Div. & Dept. of Clinical and Experimental Biomedical Sciences «Mario Serio», University of Florence, Florence, Italy

[2] Dept. of Clinical and Experimental Biomedical Sciences «Mario Serio», University of Florence, Florence, Italy

In the last decades, electromagnetotherapy generated an intense interest for the medical treatment of some pathological states related to the musculoskeletal system. In particular, extremely low frequency (ELF) electromagnetic fields (EMFs) are used to improve tissue regeneration in bone non-union fractures, to facilitate skin wound healing and to reduce pain symptomatology. This therapy represents a valid and non-invasive approach widely used to treat the area of interest limiting the adverse effects related to drug administration. The molecular mechanisms by which ELF EMFs act on cell behavior is still not completely known, but numerous and heterogeneous effects have been observed on a very large number of biological processes. These effects vary in relation to the treatment parameters and intrinsic susceptibility of specific cell lines.

In order to study the molecular mechanism by which ELF EMFs act on fibroblasts, the mouse-derived NIH3T3 cell line was chosen as the experimental model to carry out some biochemical investigations. After EMF exposure, the cells showed an increased level of ROS and a decreasing activity of the enzyme pyruvate kinase (PK), leading to a slowdown of the glycolytic flux and a redirection of glycolytic metabolites towards the pentose phosphate pathway (PPP). Hence, the results of the study define a coherent biochemical mechanism by which ELF EMFs are able to promote a shift of cell metabolism from catabolic to anabolic processes. Additional investigations such as the evaluation of reduced glutathione levels, are however necessary to confirm the mechanism.

INTRODUCTION

Extremely low frequency (ELF) electromagnetic fields (EMFs) have generated a growing interest for their use in medicine. This therapeutic treatment represents a safe, non-invasive approach, characterized by lack of toxicity and the possibility of being combined with other available therapies. Furthermore, one of the main advantages of electromagnetic therapy is the possibility of applying the treatment exclusively to the targeted area in order to minimize the adverse effects affecting non-targeted tissues and organs.

Electromagnetic therapy is successfully used for the medical treatment of several pathological conditions such as disorders related to musculoskeletal system, Parkinson's disease, multiple sclerosis [1] and, even though the biochemical and molecular basis is still unknown, the Food & Drug Administration (FDA) approved the use of ELF EMFs as safe for treating bone pathologies and delayed fractures. In fact, it has been reported that EMFs are able to promote proliferation and differentiation of osteoblasts [2]. Another common application of electromagnetic therapy is to facilitate the healing process in chronic wounds because electromagnetic treatments seem to influence the process of tissue repairing by acting on various secondary messengers [3]. From a molecular point of view, it seems that electromagnetic therapy exerts an anti-inflammatory effects in treated tissues due to a down-regulation of COX-2 expression and a lower production of PGE-2 [4].

Hence, electromagnetic therapy constitutes an adjuvant therapy and a valid alternative to use when traditional medicine do not produce any significant improvement and, for these reasons, it is necessary to increase the molecular and biochemical comprehension related to the mechanism of action of ELF EMFs on biological systems in order to

improve its therapeutic potential.

The biological effects of ELF EMFs have been investigated in several in vitro studies and results indicate that ELF EMFs have heterogeneous effects on a very large number of biological processes such as cell cycle distribution and proliferation [5, 6], cell migration [7], apoptosis [8], gene expression [9] and differentiation [10]. All of these effects vary in relation to frequency, amplitude, length of exposure and are also related to intrinsic susceptibility of different cell types. Sul et al. [11], for example, have compared the effects of electromagnetic exposure (60 Hz, 2 mT) on four kinds of human cell lines demonstrating that there is a specific cell-type response to EMFs, tightly correlated to the duration of exposure. Moreover, different effects can be observed even when similar cells are exposed to EMFs. In fact, when HaCaT and NHEK cells are exposed to EMFs (60 Hz, 1,5 mT), a G1 arrest is detected in HaCat cells, while no effects on cell proliferation and cell cycle distribution is observed in NHEK cells [12].

A lot of assumptions have been made to explain how physical stimulus is converted to chemical signal, but the transduction pathway by which EMF acts on cells, has not been elucidated. Calcium signaling plays an important role in regulating proliferation, differentiation and apoptosis and it was reported that ELF EMFs can alter the levels of cytosolic Ca2+ [13], although this effect seems to be specific to the cell type and the EMFs parameters applied. Another important molecular response to ELF EMFs is represented by an increasing level of intracellular reactive oxygen species (ROS) in cells exposed to EMFs [14]. Since ELF EMFs seems to work by affecting the redox state of cells by promoting variations of physiological ROS levels, biological processes can be influenced by the electromagnetic treatment and this aspect could provide a possible molecular mechanism to explain the beneficial effects of electromagnetic therapy. In fact, it was demonstrated that increasing levels of ROS occurred after ELF EMFs treatment, taking to the activation of the molecular events able to induce cell proliferation due to the activation of redox signals involving NFkB proteins [15].

Since ROS can act as signaling molecules deeply involved in regulating cellular processes and metabolism, via cysteine oxidation, as recently reported in literature [16, 17], the activities of the enzymes involved in the principal metabolic pathways have been evaluated in NIH3T3 cells exposed to ELF EMFs. In particular, our attention has been focused on the isoform M2 of pyruvate kinase (PKM2) because it has been described that the oxidation of Cys358 causes the inhibition of the enzyme [18]. In order to establish whether ELF EMFs can exert metabolic modifications in NIH3T3 cells, the intracellular levels of ROS, the enzymatic activity of PK, citrate synthase (CS) and the endogenous concentrations of ATP have been evaluated after EMF exposure.

MATERIALS AND METHODS

Cell cultures

Mouse embryonic fibroblasts (NIH3T3 cell line) were used as cellular model to investigate the cellular and molecular effects of ELF EMFs. Since this model system has been used in a multitude of different studies, NIH3T3 cells were chosen to conduct the investigation because it represent a well characterized cellular model. Cells were grown at 37°C, in 5% CO^2/air atmosphere, in Dulbecco's Modified Eagle Medium (DMEM) (Sigma-Aldrich) supplemented with 10% (v/v) heat- inactivated foetal calf serum (FCS) (Biowest) and 2 mM L-glutamine (Biowest). Cells were seeded (3.0×105) in 100 mm Falcon dishes and propagated every 3 days with a 0.25% trypsin solution (Sigma-Aldrich) Cells were purchased from ATCC (ATCC CRL-1658). No antibiotics were used in cell cultures. Cell cultures were periodically tested for Mycoplasma contamination.

Experimental setup for exposure cells to ELF EMFs

Cell exposure to ELF EMFs was carried out by a medical device commercially available (Easy Qs device), produced by ASAlaser (Vicenza, Italy). The source of EMFs constituted of a rectangular shaped surface applicator provided of 12 coils. Each coil generates a sinusoidal signal and magnetic flux density was longitudinally and transversely evaluated by the company that realizes the device.

In our investigations two different electromagnetic treatments were evaluated. Cells were exposed for 20 minutes to the frequencies of 25 Hz (1.62 mT) and 50 Hz (2.4 mT). During the time of exposure to EMFs, control and treated cells were kept under the same environmental conditions. Cells were seeded (2.0×105) on 60 mm Petri dishes and cultured until reaching exponential growth phase. Hence, cells were treated with EMFs and prepared for the assays.

MTT assay

MTT assay is a rapid colorimetric analysis routinely used to investigate the state of cell energy metabolism and possible cytotoxic effects. This assay is based on the principle that metabolically active cells are able to convert a yellow water-soluble tetrazolium salt, 3-(4,5-dimethylthazolk-2-yl)-2,5-diphenyl tetrazolium bromide) (MTT), into a purple colored formazan product by mitochondrial succinate dehydrogenases (SDH). MTT assay was also used to evaluate the enzymatic activity of SDH because it has been demonstrated that SDH activity and MTT reduction were closely related [19]. Cells were exposed to EMFs and MTT assay was performed immediately after the end of treatment and 24 hours later. Cells were incubated for 40 minutes with 1 mM thiazolyl blue tetrazolium bromide (Sigma-Aldrich). At the end of incubation, the medium was removed and DMSO was added in each plate to dissolve formazan crystals. The absorbance signal was read at 570 nm by a microplate reader (Infinite M200PRO, Tecan). The background absorbance was read at 630 nm and subtracted from signal absorbance to obtain normalized absorbance values.

Immunofluorescence analysis

Cells were fixed on the cover slides using

4% formalin for 10 minutes, permeabilized for 5 minutes with 0,1% Triton X-100 and blocked for 1 hour with 3% FBS in PBS solution at room temperature. For tubulin detection, mouse anti α-tubulin antibody conjugated with Alexa Fluor 488 (1:500; Life Technologies) was incubated for 2 hours at room temperature. Actin was stained for 20 minutes with CF594 conjugated Phalloidin (1:40; Biotium), at room temperature. Nuclei were stained by Fluoroshield with DAPI mountant (Sigma-Aldrich).

Measurement of intracellular ROS

The level of intracellular ROS was quantified by fluorescence with 2'-7,-dichlorofluorescein diacetate (DCFH2-DA, Sigma-Aldrich, Italy), as described by Bass et al. [20]. Before ELF EMFs exposure, cells were incubated with DCF-DA (20 μM) for 1 hour at 37°C. After treatment to EMFs, cells were immediately washed twice with PBS and the relative levels of fluorescence were quantified by a multi-detection microplate reader (Infinite M200PRO, Tecan; λex=485 nm; λem=535 nm). Fluorescence values were reported as mean of fluorescence intensity. Hydrogen peroxide was used as a positive control (80 μM, for 30 minutes).

Experimental setup for enzymatic activities assays

Cells were treated with EMFs and prepared for biochemical investigations which have been conducted 5 and 24 hours after EMFs exposure.

The enzymatic activities of pyruvate kinase (PK) and citrate synthase (CS) have been evaluated in order to detect a possible alteration in cell metabolism following treatment with EMFs. In order to verify a possible role of ROS in regulating enzymatic activities, DASA-10 (Sigma-Aldrich), diamide (Sigma-Aldrich) and H_2O_2 (Sigma-Aldrich) were used in enzymatic activities evaluations. DASA-10 is a little molecule that binds to the isoform M2 of PK and cover cys358, maintaining the - SH of cys358 in its reduced state, and then, protecting PKM2 (PKM2) from ROS-induced inhibition [18]. In our experiment DASA-10 was used at 20 μM for 1 hour before treatments. Some further control groups were establish in order to assess the protective action of DASA-10 in oxidative conditions and these groups are listed below:

- Control cells were treated with H_2O_2 (80 μM) for 40 minutes.
- Control cells were treated with diamide (250 μM) for 15 minutes.
- Control cells were treated wit DASA-10 (20 μM) for 1 hour and then with H_2O_2 (80 μM) for 40 minutes.
- Control cells were treated with DASA-10 (20 μM) for 1 hour and then with diamide (250 μM) for 15 minutes.

The activities assays were repeated after incubating the samples for 2 hours with 2 mM dithiothreitol (DTT).

This experimental design was also utilized in the evaluation of ATP levels.

Cell lysis

Cell lysis was performed in cold buffer (50 mM Tris-HCl pH 7.4) containing Sigma protease inhibitors mix (1:100, v/v), DTT (5 mM), or not DTT. After 30 min of incubation on ice, lysates were sonicated (three short bursts) and centrifuged in a microcentrifuge for 30 min at 12.000 g (4°C). Supernatants were used for the

Fig 1:

MTT assay in NIH3T3 cells exposed to EMFs was performed immediately after the exposure (T_0) and after 24 hours. Two different EMF treatments were compared (25 Hz and 50 Hz). Results are expressed as a percentage of the absorbance signal of control cells (indicated as 100%).

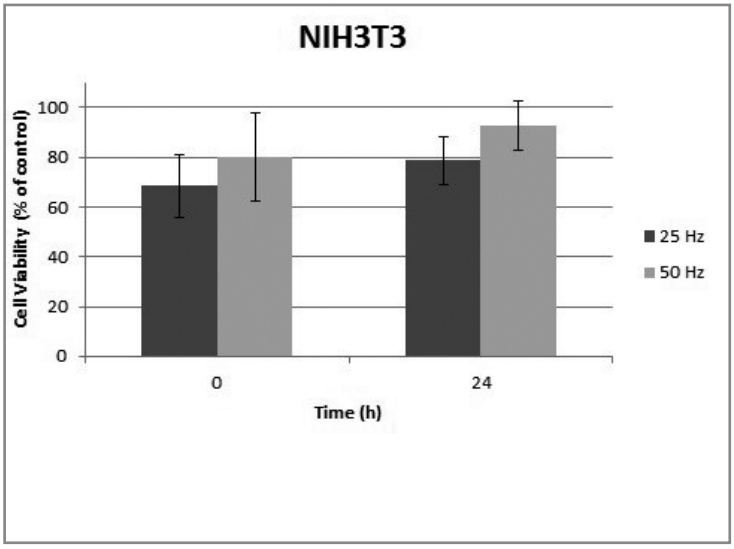

Fig 2:

Immunofluorescent analysis of cytoskeleton architecture in NIH3T3. Upper row: fluorescent microscopy of F-actin stained with Phalloidin (red) and nuclei with DAPI (blue). Cells were fixed 24 hours after EMF treatment. Lower row: fluorescent microscopy of α-tubulin (green) and nuclei with DAPI (blue). Images were collected at 100x magnification.

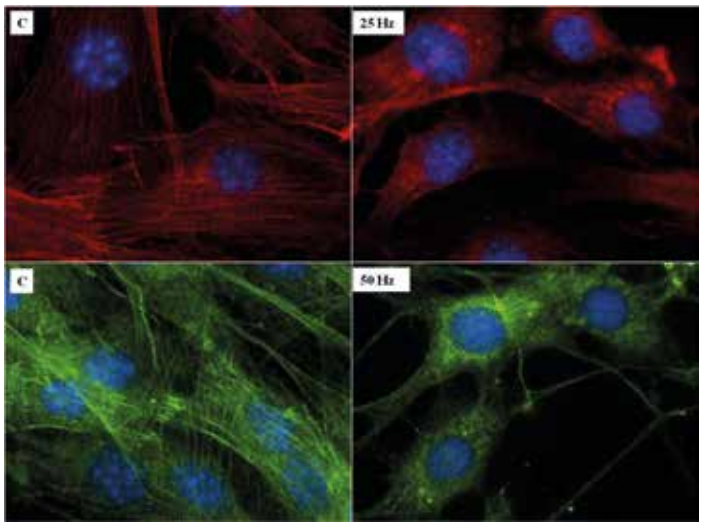

evaluation of enzymatic activities with respect to proteins content.

Determination of total proteins content

Total proteins concentration was determined spectrophotometrically according to the Bradford method [21], using a reagent produced by Sigma-Aldrich.

Pyruvate kinase (PK) activity (EC 2.7.1.40)

The enzymatic assays were performed at 30°C spectrophotometrically using an UV-2100 spectrophotometer (Shimadzu). PK activity was determined according to Hess and Wieker [22], with slight modifications, monitoring the NADH oxidation at 340 nm. The values of 6.22 mM-1 cm- 1 and 14.15 mM-1 cm-1 are considered to be the NADH molar extinction coefficients. One unit of activity is defined as that quantity of enzyme which transforms one µmole of substrate in one minute, at 30°C.

The assay mixture consisted of 50 mM triethanolamine (pH 7.6), 8 mM MgSO4, 5 mM EDTA, 75 mL KCl, 1.5 mM ADP, 0.15 mM NADH, 5 µg/ml lactate dehydrogenase. The reaction was started by adding the substrate (0.8 mM phosphoenolpyruvate).

Citrate synthase (CS) activity (EC 2.3.3.1)

The citrate synthase is the key enzyme of the Krebs cycle ant it catalyzes the synthesis of citric acid from oxaloacitic acid and acetyl-CoA. Citrate synthase activity was evaluated in order to establish Krebs cycle functionality. For the determination of CS activity, the citrate synthase assay kit (Sigma-Aldrich; CS0720) was used.

ATP bioluminescent assay

The possible effects of EMFs exposure on cellular energy metabolism were evaluated by measuring the levels of adenosine 5'-triphosphate (ATP). For the quantitative determination of intracellular ATP levels, bioluminescent assay kit (Sigma-Aldrich; FLAA) was used. The assay is based on the luciferin-luciferase reaction that utilizes ATP to oxidize D-luciferin producing adenyl-luciferin. During the enzymatic reaction, ATP is consumed and light is emitted. Hence, the light emitted is proportional to ATP content.

Statistical analysis

Statistical analysis was calculated based on two-tailed t-test using Prism Graphpad. Differences were considered statistically significant for $P < 0.05$. All data are presented as mean ± DS of thee independent experiments.

RESULTS

MTT assays

MTT assay was performed in order to estimate cell metabolic activity and possible cytotoxic effects of EMFs on cells. NIH3T3 cells were treated with ELF EMF radiation for 20 minutes and the assays were performed immediately at the end of EMF exposure (T_0) and after 24 (T_{24}). The results are reported in figure 1 and they indicate that the EMF effects on cell viability were quite heterogeneous with regards to exposure parameters. In fact, when cells were treated with 50 Hz EMFs, no significant changes in cell viability have been observed, whereas cells treated with 25 Hz EMFs showed a reduction in the absorbance signal immediately after the end of treatment. Nevertheless, it should be noted that this difference resulted less marked after 24 hours, indicating a recovery in cell metabolism or in the cell number.

Cytoskeleton

Cytoskeleton is the fundamental structure that allows both cellular movement and shape maintaining and it is also fundamental in coordinating vesicles trafficking and the organelles motion. Immunofluorescence analysis of the main cytoskeleton components (actin microfilaments and microtubules) has been conducted 24 hours after EMF treatment in order to evaluate possible morphological changes after EMF treatment. In figure 2 immunofluorescence results are reported. In control cells (left column) cytoskeleton components appear well defined, showing actin microfilaments homogeneously distributed and a well organized pattern for microtubules. In treated cells (25 Hz for actin and 50 Hz for tubulin), alterations in cytoskeleton structure are evident for actin microfilaments and for microtubules: the precise organization found in control cells is totally lost and cytoskeleton components appear completely unstructured.

Fig 3:

Evaluation of intracellular ROS levels in NIH3T3 cells. ROS production results higher in exposed cells (25 Hz and 50 Hz) rather than control cells. H_2O_2-treated cells were used as positive control (80 µM for 30 minutes).

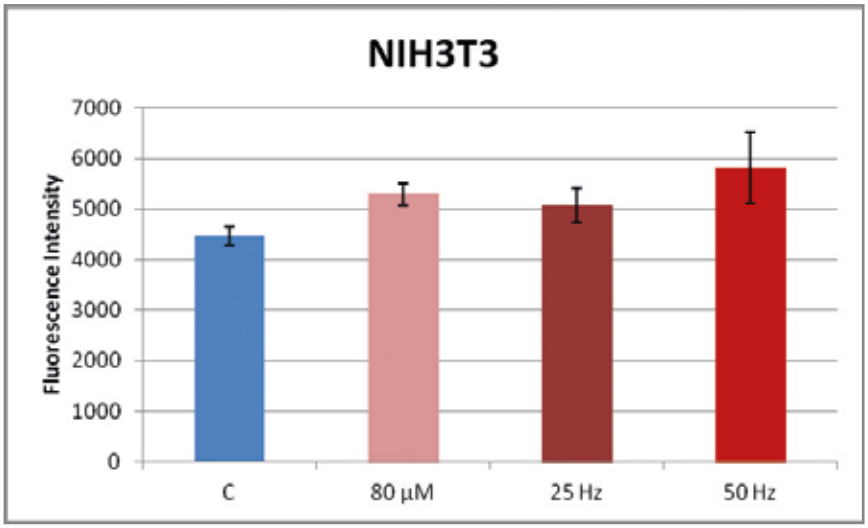

Evaluation of ROS and enzymatic activities

Since it has been reported that ELF EMFs could act on cells, inducing an increased intracellular level of ROS [23], measurements of ROS production were conducted after EMFs exposure using $DCFH_2$-DA assay. NIH3T3 cells were labeled with $DCFH_2$-DA, as previously described in "Materials and Methods" section and then cells were exposed for 20 minutes to EMFs at 25 Hz (1.62 mT) and 50 Hz (2.4 mT). Results show that ROS production is significantly higher in cells exposed to EMFs (Fig. 3) and the increasing fluorescence of DCF is registered in both treatments. In particular, NIH3T3 result more susceptible when exposed at 50 Hz EMF (2.4 mT) rather than 25 Hz EMF (1.62 mT).

Enzymatic activities assays

NIH3T3 cells express the M2 isoform of PK, an homotetramer composed of four 56 kDa subunits containing three cysteine residues; Cys^{31}, Cys^{358}, Cys424. Cys^{358} is located in a beta-barrel that includes residues essential for the catalytic activity. Recent literature widely described how the oxidation of Cys^{358} causes the inhibition of PKM_2 and how this inhibitory effect could be reverted using reductive agents, such as DTT [18]. Since evaluations of intracellular ROS level demonstrate an increasing ROS production in cells exposed to EMFs, an inhibitory effect on PK activity following EMF treatment was assumed.

In figure 4 have been reported the specific activity levels of PK. Diamide and H_2O_2 have been used as positive control of Cys358 oxidation of PKM2; H_2O_2 causes oxidation due to ROS generation, whereas diamide is an oxidant compound which act selectively on -SH groups of proteins. DASA- 10 is a small molecule used as a protective agent for Cys^{358} oxidation of PKM2 because it binds the subunit of PKM2 at the level of Cys^{358}, preventing Cys^{358} oxidation and the consequent inhibitory effect on PKM2. Hence, cells treated with DASA-10 constitute a negative control.

Cells treated with DASA-10 (Dasa-10 group) show an higher PK activity rather than control cells and this effect can be explained due to the protective action exerted by DASA-10 during the cell lysis because lysis buffer do not contain any antioxidant agent (DTT). The specific activity of PK in cells treated with H_2O_2 or diamide (H_2O_2 group and diamide group) appears lower than that of control cells, indicating that an inhibitory effect of PKM2 occurred. When cells are pretreated with DASA-10 and then exposed to H_2O_2 (or diamide), the specific activity of PK results comparable with "DASA-10" group. Once again, data indicate that DASA-10 preserve the activity of PKM2, protecting Cys^{358} from oxidation. The activity level of PK in cells exposed to 25 Hz results similar to those of positive control (H_2O_2 group and diamide group). When cells are pretreated with DASA-10 and then exposed to 25 Hz (DASA-10_25 Hz), PK activity results comparable to "DASA-10_H_2O_2" group, indicating that EMFs and H_2O_2 could act through the same effector substance, ROS. As regards "50 Hz" and "50 Hz_DASA-10" groups, the specific activities level are comparable to those observed in "25 Hz" and "25 Hz_DASA" groups. In order to establish whether could be possible restoring PKM2 activity using reductive agents (DTT) which could reduce Cys^{358} of PKM2, every experimental group was evaluated immediately after cell lysis (no DTT), and after an incubation of 2 h with DTT 2 mM,. When PKM2 was inhibited by H_2O_2, diamide and EMF treatments (both 25 and 50 Hz), it was possible to restore its specific activity after incubation with DTT, showing activity values comparable to control group. The protective action exerts by DASA- 10 on the activity of PKM2 and its restoring following DTT incubation demonstrate that the inhibition of PKM2 is attributable at least in part to the oxidation of Cys^{358}. Moreover, results indicate that EMF treatments could act on the activity

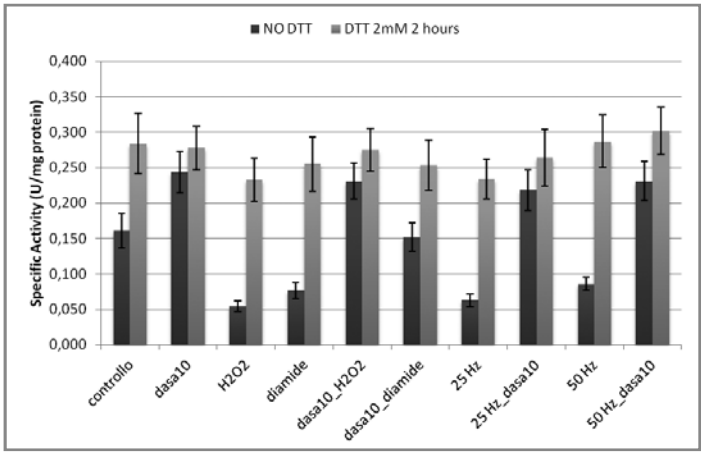

Fig 4:
Specific activities of PK in NIH3T3, evaluated 5 hours after treatments. Control: No treated cells. DASA- 10: Cells treated with DASA-10 (20 uM for 1 h). H_2O_2: Cells treated with H_2O_2 (80 uM for 40 min). Diamide: Cells treated with diamide (250 uM for 15 min). Dasa10_H_2O_2: Cells pre-treated with DASA-10 (20 uM for 1 h) and then exposed to H_2O_2 (80 uM for 40 min). Dasa10_ Diamide: Cells pre-treated with DASA-10 (20 uM for 1 h) and then exposed to diamide (250 uM for 15 min). 25 Hz: cells exposed for 20 minutes to ELF EMFs at 25 Hz. 25 Hz_DASA-10: Cells pre-treated with DASA-10 (20 uM for 1 h) and then exposed to EMFs at 25 Hz. 50 Hz: cells exposed for 20 minutes to ELF EMFs at 50 Hz. 50 Hz_DASA-10: Cells pre-treated with DASA-10 (20 uM for 1 h) and then exposed to EMFs at 50 Hz. The activity of PK was evaluated in the cellular samples immediately after lysis (no DTT; black bar) and after DTT incubation (2 mM, 2 hours) (grey bar).

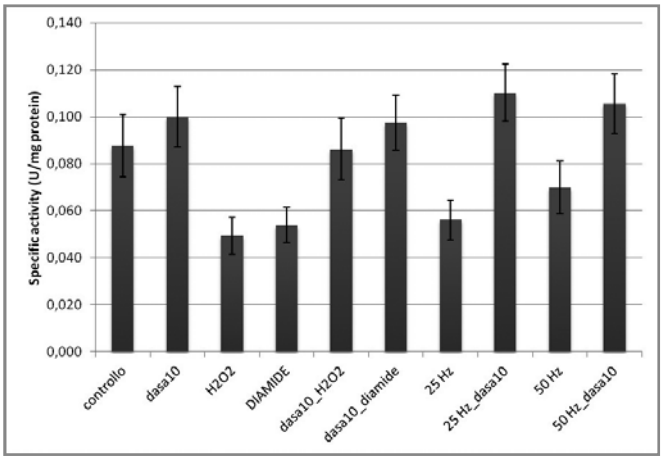

Fig 5:
Specific activities of CS in NIH3T3, evaluated 5 hours after treatments. Control: No treated cells. DASA- 10: Cells treated with DASA-10 (20 uM for 1 h). H_2O_2: Cells treated with H_2O_2 (80 uM for 40 min). Diamide: Cells treated with diamide (250 uM for 15 min). Dasa10_H_2O_2: Cells pre-treated with DASA-10 (20 uM for 1 h) and then exposed to H_2O_2 (80 uM for 40 min). Dasa10_ Diamide: Cells pre-treated with DASA-10 (20 uM for 1 h) and then exposed to diamide (250 uM for 15 min). 25 Hz: cells exposed for 20 minutes to ELF EMFs at 25 Hz. 25 Hz_DASA-10: Cells pre-treated with DASA-10 (20 uM for 1 h) and then exposed to EMFs at 25 Hz. 50 Hz: cells exposed for 20 minutes to ELF EMFs at 50 Hz. 50 Hz_DASA-10: Cells pre-treated with DASA-10 (20 uM for 1 h) and then exposed to EMFs at 50 Hz.

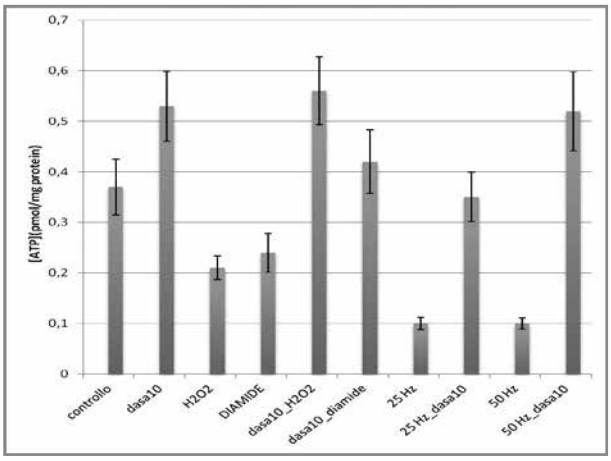

Fig 6:
ATP concentrations (pmol/mg protein) in NIH3T3 cells, evaluated 5 hours after treatments. Control: No treated cells. DASA-10: Cells treated with DASA-10 (20 uM for 1 h). H_2O_2: Cells treated with H_2O_2 (80 uM for 40 min). Diamide: Cells treated with diamide (250 uM for 15 min). Dasa10_H_2O_2: Cells pre-treated with DASA-10 (20 uM for 1 h) and then exposed to H_2O_2 (80 uM for 40 min). Dasa10_Diamide: Cells pre-treated with DASA-10 (20 uM for 1 h) and then exposed to diamide (250 uM for 15 min). 25 Hz: cells exposed for 20 minutes to ELF EMFs at 25 Hz. 25 Hz_DASA-10: Cells pre-treated with DASA-10 (20 uM for 1 h) and then exposed to EMFs at 25 Hz. 50 Hz: cells exposed for 20 minutes to ELF EMFs at 50 Hz. 50 Hz_DASA-10: Cells pre-treated with DASA-10 (20 uM for 1 h) and then exposed to EMFs at 50 Hz.

level of PK with a mechanism ROS- mediated.
The inhibition of PKM2 mediated by the oxidation of Cys^{358} implies a deficiency of pyruvate, resulting in a lower production of ATP by Krebs cycle. Therefore, the activity levels of PK have been related to the specific activity of CS in order to evaluate the functionality of Krebs cycle. CS, key enzyme of Krebs cycle, catalyzes the condensation reaction of one molecule of acetyl-CoA and
a molecule of oxalacetate to form citrate, triggering Krebs cycle. The activity levels of CS are reported in figure 5.
Similarly as for PK activity, the specific activity of CS in cells treated with EMFs (both 25 Hz and 50 Hz) show groups are comparable to "DASA-10_H2O2" and "DASA-10_diamide". Here again, when cells are pretreated with DASA-10 and then exposed to EMFs (both 25 Hz and 50 Hz), the specific activity levels of CS are comparable to those of control cells.

ATP concentrations

Intracellular ATP concentration was measured in order to evaluate if the variations observed in PK and CS activity levels may lead to variations of ATP contents. Results are presented in figure 6.
When cells are exposed to EMFs, the concentration of ATP is significantly reduced (both 25 Hz and 50 Hz groups). When cells are pretreated with DASA-10, ATP concentration results comparable to control cells (25 Hz_ DASA-10 group) and higher than control cells (50 Hz_DASA-10 group).

DISCUSSION

The MTT assay is a colorimetric assay for assessing cell metabolic activity. Tetrazolium dye essays can also be used to measure cytotoxicity (loss of viable cells) or cytostatic activity (shift from proliferation to quiescence) due to different causes.
The results of MTT essays performed on samples exposed to EMFs showed a lower absorbance in comparison with untreated controls. The difference was more evident immediately after the exposure than at T=24h. The absorbance is related to the number of cells and also to their metabolic state. Seeing that after 24h there is a partial recovery, we hypothesized that the absorbance decrease could indicate a temporary metabolic slowdown or a temporary shift from proliferation to quiescence rather than a lower cell viability.
Immunofluorescence experiments, performed staining actin and tubulin, showed that the organization of the main cytoskeletal elements was altered and both microfilaments and

microtubules seemed depolymerized . These cytoskeletal alterations are in agreement with the increase in ROS concentration found after exposure to EMFs and provide important morphological information about the possibility that ROS could act also promoting the cytoskeleton remodeling, enriching the variety of molecular effects exerted by EMF on cells. In fact, it has been reported that ROS could affect the balance between polymerization/depolymerization of actin filaments and microtubules [25]. In particular, it has been reported that an increased level of intracellular ROS seems to be related to a lower polymerization of cytoskeletal elements through effects on PKM2 [26]. Our experimental results are consistent with the literature, because we found that cells exposed to EMFs present an increased level of ROS, enhanced depolymerization and an active remodeling of cytoskeleton. Hence, a molecular mechanism by which EMF can act on the cytoskeleton remodeling of cells is proposed.

PK is the enzyme that catalyzes the final reaction of glycolysis where a phosphate group is transferred from phosphoenolpyruvate (PEP) to ADP, yielding to the formation of one molecule of pyruvate and one molecule of ATP. There are several isoforms of PK and PKM2 isoform is highly susceptible to oxidation at the level of Cys^{358}. The oxidation of Cys^{358} results in the inhibition of the catalytic activity of the enzyme, promoting a slowdown of the glycolytic flux. In fact, since the PKM2 activity results inhibited by the oxidation of Cys^{358}, pyruvate is not synthesized and the

glycolytic flux slows down, promoting the accumulation of metabolites that are diverted to the pentose phosphate pathway (PPP), causing a metabolic shift toward anabolic processes. These considerations indicate that the redox state of the cells represent a way of regulating the enzymatic reactions involved in cellular metabolism [24]. In fact, cells with high anabolism (e.g. neoplastic cells, embryonic cells and cells involved in repair processes) are characterized by metabolic regulation mechanisms strictly related to their redox state and our experimental evidences support this kind of metabolic regulation also in NIH3T3 cells.

According to literature, our results indicate an increased intracellular ROS level after EMF treatments [14] and, since NIH3T3 cells express the isoform M2 of PK, a metabolic shift toward anabolism has been hypothesized.

In fact, our findings demonstrated that PK activity decreased after EMF exposure (25 Hz and 50 Hz), while ROS levels increased, similarly to what happens as a result of oxidative stress (H_2O_2) . The same effect was observed when cells were treated with diamide, a chemical compound used for the specific oxidation of -SH groups in proteins. From these observations we can assume that the mechanism by which ROS and diamide act, is similar and it includes the oxidation of Cys^{358}, promoting the inhibition of PKM2. These considerations are supported by the results obtained when cells were pre-treated with DASA-10, a specific molecule used to protect the oxidation of Cys358 in PKM2: cells pre-treated with DASA-10 and then exposed EMFs, or to oxidant treatments, did not show reduced PKasic activity compared with controls. Moreover, PKasic activity resulted totally restored after DTT incubation, showing values of specific activity comparable to those of control.

The decrease in PKM2 activity fits with the depolymerization of cytoskeleton: recently, an interaction between PKM2 and the elements of cytoskeleton has been demonstrated [26].

Pyruvate is a key metabolite connecting different metabolic pathways such as glycolysis, gluconeogenesis, Krebs cycle, fatty acids synthesis. In fact, it can be converted in acetyl-CoA by pyruvate dehydrogenase and it can be diverted towards Krebs cycle and fatty acid synthesis. Therefore, pyruvate provides the substrate of CS, the key enzyme of Krebs cycle, which catalyzes the condensation reaction of a molecule of acetyl-CoA and a molecule of oxalacetate to form citrate, triggering Krebs cycle. In this context, the activity level of PK is strictly correlated to CS activity and ATP production.

Indeed, the results of the experiments showed that in cells exposed to EMFs a decrease in CS activity also occurs. All that, prompted us to hypothesize that also a slowdown of the Krebs cycle, with consequent decrease in ATP production, could occur. This hypothesis was then supported by data concerning ATP concentration: samples exposed to EMFs showed ATP levels markedly lower than controls. Moreover, the results obtained with the MTT essays reinforce our hypothesis of a metabolic shift following EMF treatments. In fact, MTT was performed not only to evaluate possible cytotoxic effects of EMF treatment, but also to provide a general evaluation of the activity of succinate dehydrogenase (SDH), the common enzyme between Krebs cycle and the electron transport chain. Although MTT assay for SDH activity results less accurate than classic methods used in enzymatic activity determinations, it provides a first assessment of the electron transport chain efficiency that is strictly related to the production of ATP. The results of the MTT assay are consistent with a framework of Krebs cycle slowdown, decrease in CS activity, lower efficiency of the electron transport chain and decrease in ATP production.

To sum up, our results demonstrate a molecular mechanism by which ELF EMFs are able to promote a metabolic shift toward anabolic processes in NIH3T3 cells, inducing an increased level of intracellular ROS first, and a reduced activity of PKM2 then. The slowdown of glycolytic flux causes the accumulation of glycolytic intermediates which are diverted to PPP, a metabolic pathway with anabolic character. In fact, PPP promotes the production of 5-carbon sugars, required for nucleotides synthesis in cell proliferation, and generation of reduced NADPH, the cofactor implicated in anabolic processes such as lipid synthesis. Moreover, NADPH is also involved in regeneration of glutathione (GSH), constituting the antioxidant system implicated in maintaining a basal level of ROS inside the cells. As a result, the effects of ELF EMFs are assumed to be temporary, because the increased ROS level following EMF treatment is constrained by the antioxidant system, that is supported by the production of NADPH through PPP with a positive feedback.

This mechanism, that starts as response to a

stress, could trigger a series of anabolic pathways in cells expressing PKM2, which are generally characterized by high anabolic rates.

In conclusion, in NIH3T3 fibroblasts, and probably in all the cells expressing PKM2, ELF EMFs induce a shift of the cell metabolism from catabolic to anabolic processes via a temporary increase in the ROS levels that can be controlled by the antioxidant system through a feedback mechanism.

REFERENCES

1. Rosch P.J., Markov M.S. Bioelectromagnetic Medicine. NY: Marcel Dekker, 2004.
2. Wei Y., Xiaolin H., Tao S. Effects of extremely low frequency-pulsed electromagnetic field on osteoblast-like cells. Electromagn Biol Med. 2008; 27(3): 298-311.
3. Costin G.E., Birlea S.A., Norris D.A. Trends in wound repair: cellular and molecular basis regenerative therapy using electromagnetic fields. Curr Mol Med. 2012; 12: 14-26.
4. Patruno A., Amerio P., Pesce M., Vianale G., Di Luzio S., Tulli A., Franceschelli S., Grilli A., Muraro R., Reale M. Extremely low frequency electromagnetic fields modulate expression of inducible nitric oxide synthase, endothelial nitric oxide synthase and cyclooxygenase-2 in the human keratinocyte cell line HaCat: potential therapeutic effects in wound healing. Br J Dermatol. 2010; 162(2): 258-266.
5. Ruiz Gómez M.J., De la Peña L., Pastor J.M., Martínez Morillo M., Gil L. 25 Hz electromagnetic field exposure has no effect on cell cycle distribution and apoptosis in U-937 and HCA-2/1cch cells. Bioelectrochemistry. 2000; 53:137-140.
6. Tsai M.T., Chang W.H., Chang K., Hou R.J., Wu TW. Pulsed electromagnetic fields affect osteoblast proliferation and differentiation in bone tissue engineering. Bioelectromagnetics. 2007; 28: 519-528.
7. Sunkari V.G., Aranovitch B., Portwood N., Nikoshkov A. Effects of a low-intensity electromagnetic field on fibroblast migration and proliferation. Electromagn Biol Med. 2011; 30(2): 80-85.
8. Basile A., Zeppa R., Pasquino N., Arra C., Ammirante M., Festa M., Barbieri A., Giudice A., Pascale M., Turco M.C., Rosati A. Exposure to 50 Hz electromagnetic field raises the levels of the anti-apoptotic protein BAG3 in melanoma cells. J Cell Physiol. 2011; 226: 2901-2907.
9. Mayer-Wagner S., Passberger A., Sievers B., Aigner J., Summer B., Schiergens T.S., Jansson V., Müller P.E. Effects of low frequency electromagnetic fields on the chondrogenic differentiation of human mesenchymal stem cells. Bioelectromagnetics. 2011; 32: 283-290.
10. Ross C.L., Harrison B.S. An introduction to electromagnetic field therapy and immune function: a brief history and current status. J Sci Appl: Biomed. 2015; 3(2): 18-29.
11. Sul A.R., Park S.N., Suh H. Effects of sinusoidal electromagnetic field on structure and function of different kinds of cell lines. Yonsey Med J. 2006; 47: 852-861.
12. Huang C.Y., Chuang C.Y., Shu W., Chang C.W., Chen C.R., Fan T.C., Hsu I.C. Distinct epidermal keratinocytes respond to extremely low-frequency electromagnetic fields differently. PLoS One. 2014; 9(11): e113424.
13. McCreary C.R., Dixon S.J., Fraher L.F., Carson J.J.L., Prato F.S. Real-time measurement of cytosolic free calcium concentration in Jurkat cells during ELF magnetic field exposure and evaluation of the role of cell cycle. Bioelectromagnetics. 2006; 27: 354-364.
14. Consales C., Merla C., Marino C., Benassi B. Electromagnetic fields, oxidative stress and neurodegeneration. Int J Cell Biol. 2012; vol 2012. Article ID 683897.
15. Wolf F.I., Torsello A., Tedesco B., Fasanella S., Boninsegna A., D'Ascenzo M., Grassi C., Azzena G.B., Cittadini A. 50-Hz extremely low frequency electromagnetic fields enhance cell proliferation and DNA damage: possible involvement of a redox mechanism. Biochim Biophys Acta. 2005; 1743: 120-129.
16. Sarsour E.H., Kumar M.G., Chaudhuri L., Kalen A.L., Goswami P.C. Redox control of the cell cycle in health and disease. Antioxid Redox Signal. 2009; 11(12): 2985-3011.
17. Paulsen C.E., Carroll K. Cysteine-mediated redox signaling: chemistry, biology and tool for discovery. Chem Rev. 2013; 113(7): 4633-4679.
18. Anastasiou D., Poulogiannis G., Asara J.M., Boxer M.B., Jiang J.K., Shen M., Bellinger G., Sasaki A.T., Locasale J.W., Auld D.S, Thomas C.J., Vander Heiden M.G., Cantley L.C. Inhibition of Pyruvate Kinase M2 by Reactive Oxygen species contributes to cellular antioxidant responses. Science. 2011; 334(6060): 1278-1283.
19. Dong L.F., Low P., Dyason J.C., Wang X-F, Prochazka L., Witting P.K., Freeman R., Swettenham E., Valis K., Liu J., Zobalova R., Turanek J., Spitz D.R., Domann F.E., Scheffler I.E., Ralph S.J., Neuzil J. -Tocopheryl succinate induces apoptosis by targetin ubiquinon-binding sites in mitochondrial respiratory complex II. Oncogene. 2008; 27: 4324-4335.
20. Bass DA, Parce J.W., Dechatelet L.R., Szejda P., Seeds M.C., Thomas M. Flow cytometric studies of oxidative product by neutrophils: a graded response to membrane stimulation. J Immunol. 1983;130(4):1910-1917.
21. Bradford M. A rapid and sensitive method for the quantification of microgram quantities of protein utilizing the principle of protein-day binding. Anal Biochem. 1976; 72: 248-254.
22. Hess B., Wieker H.J. Methods for determination of enzyme activity: pyruvate kinase. In Bergmeyer H.U., Methods of enzymatic analysis, 2 Edn, Vol 2, Academic Press, New York, 1974; 778-783.
23. Palumbo R., Capasso D., Brescia F., Mita P., Sarti M., Bersani F., Scarfi M.R. Effects on apoptosis and reactive oxygen species formation by Jurkat cells exposed to 50 Hz electromagnetic fields. Bioelectromagnetics. 2006; 27(2): 159-162.
24. Ralser M., Wamelink M.M., Kowald A., Gerisch B., Heeren G., Struys E.A., Klipp E., Jakobs C., Breitenbach M., Lehrach H., Krobitsch S. Dynamic rerouting of the carbohydrate flux is key to counteracting oxidative stress. J Biol. 2007; 6(4): 10.
25. Wilson C., González-Billault C. Regulation of cytoskeletal dynamics by redox signaling and oxidative stress:implications for neuronal development and trafficking. Front Cell Neurosci. 2015; 9: 381.
26. Gupta V., Bamezai RNK. Human pyruvate kinase M2: a multifunctional protein. Protein Sci. 2010; 19:2031-2044.